Determination of Stress-Related Properties of Blood Vessel Wall Phantoms Using Endoscopic Optical Coherence Tomography

S. V. Frolov[1], A. Yu. Potlov[2],
Tambov State Technical University
Tambov, Russia
[1]sergej.frolov@gmail.com, [2]zerner@yandex.ru

S. G. Proskurin[3], S. V. Sindeev[4]
Tambov State Technical University
Tambov, Russia
[3]spros@tamb.ru, [4]ssindeev@yandex.ru

***Abstract*— Method for determination of the Young's modulus and the Poisson's ratio for biological tissues investigated using endoscopic optical coherence tomography with a forward-side probe is described. Application examples of this strain elastography method are presented.**

Keywords*— optical coherence tomography; elastography; blood vessel wall phantoms; endoscopy; forward-side probes

I. INTRODUCTION

Endoscopic optical coherence tomography (OCT), as well as traditional OCT, has a micron spatial resolution and a high rate of obtaining structural images. However, an endoscopic probe with several meters length and only a few millimeters thick significantly expands the areas of possible application of this biomedical imaging method [1–4].

There are several biomedical OCT applications for cardiovascular system state estimation [2–6]: diagnosis of atherosclerotic vascular disease, supervisory control over rotational atherectomy (evacuation atherosclerotic deposits from vessel walls), evaluation of the correctness of stent deployment, determination of stress-related properties of blood vessel walls. In all these cases, the sample arm of the OCT-system is removable and is made as endoscopic probe.

The usage of endoscopic OCT for the diagnosis of atherosclerotic lesions of the walls of blood vessels makes it possible to differentiate many specific features of atherosclerotic plaques, in particular to isolate fat components, calcium, cholesterol crystals, macrophage aggregates, hemic calculus etc. In general terms, endoscopic OCT makes it possible to distinguish types of atherosclerotic plaques, which is important for the correct diagnosis and subsequent treatment order [2, 5–8].

The usage of endoscopic OCT to supervisory control over rotational atherectomy was made possible by combining the OCT probe and the cutting blade in a single catheter [1–3]. This technology allows visualizing the vessel walls during the procedure for evacuation atherosclerotic deposits. It provides additional information useful for the surgeon for the convenience evacuation atherosclerotic deposits. This approach significantly reduces the likelihood of accidental damage of blood vessel walls during the rotational atherectomy process.

Evaluation of the correctness of stent deployment using the endoscopic OCT involves obtaining a series of structural images for various sections of the artery and stent inside it [1, 4, 6–7]. This approach allows to evaluate (after the event) on the effectiveness of the stent deployment in an affected vessel and is used instead of angiography or as a complementary method.

Endoscopic OCT also is one of the promising methods of obtaining medical information about stress-related properties of the blood vessel walls. Analysis of structural OCT images before and after compression makes it possible to estimate even minor strain in investigated biological tissue. These deformations values, as well as the magnitude of the deforming force and the area of its impact made can be used to estimation of the Young's modulus and Poisson's ratio for investigated biological tissue. This technology is named optical coherence elastography or strain (the deforming impact, as a rule, is dynamic) elastography base on OCT [2–6].

The purpose of this work is to increase the efficiency and reliability of the stress-related properties evaluation for blood vessels using strain elastography based on endoscopic OCT. The novelty of the method are usage a pulse wave as a deforming force and analysis of structural OCT images before and after compression using test points for a set of convex hulls.

II. MATERIALS & METHODS

The proposed method for stress-related properties evaluation for blood vessels is that. Endoscopic OCT system with forward-side probe is used for obtaining structural OCT images of the wall of the investigated relatively large blood vessel at the moments of systole and diastole. The obtained structural images for noise removal are filtering in the temporal and frequency domains [9, 10]. Then, the displacements of the light and dark areas on the structural image of the strained investigated blood vessel are determined with respect to its initial state (i.e., diastole OCT image). Displacements below the threshold level and the displacement at the border of the image are removed. Convex hulls are formed for the remaining

978-1-5386-5824-6/18/$31.00 ©2018 IEEE

regions of displacements. Test points for convex hulls are defined and pairwise grouped. The deformations (as a result of pulse wave impact) in the investigated blood vessel wall are estimated as displacement vectors for each of the pairs of test points [9].

The Young's modulus, E, is calculated as follows:

$$E = \frac{F \cdot l}{S \cdot \Delta l},$$

where F – normal component of the deforming force, S – the area under deforming force impact, l – longitudinal dimension of the deformed area, Δl – longitudinal displacements of the internal structures of the blood vessel.

Systolic P_{SYS} and diastolic P_{DIA} blood pressures are physical quantities equal to the forces with which the blood impact per unit area of the vessel wall perpendicular to it at the moments of systole and diastole. Therefore, the normal component of the deforming force can be approximately calculated as:

$$F = P_{SYS} - P_{DIA}.$$

Note that in order to increase the accuracy of calculations is possible to find F using a common or local hemodynamic numerical model.

The area S under deforming force impact is considered equal to the full scan area of the endoscopic OCT system [9] being that the pulse wave is used as the deforming force.

Longitudinal displacements Δl of the internal structures of the investigated blood vessel are calculated as projections of displacement vectors for each pair of test points per ordinate axis. The longitudinal dimensions l of the deformed region are the result of the combination of these projects.

Poisson's ratio, μ, is calculated by the following formula:

$$\mu = \left| \frac{\Delta d \cdot l}{d \cdot \Delta l} \right|,$$

where Δd – transversal displacements of the internal structures of the investigated blood vessel, d – transversal dimension of the deformed area [9].

The parameter Δd is calculated by analogy with parameter Δl, with the only difference that is used projections of displacement vectors not on the ordinate axis, but on the abscissa axis for each pair of test points. The transverse dimensions d of the deformed area calculate by analogy with l, as a result of combining the projections (but, on the abscissa axis in this case).

III. Results & Discussion

The functional capability of the proposed method was evaluated out using a series of experiments with tissue-equivalent phantoms of soft biological tissues [9, 12–14]. The matrix of each phantom was made of a transparent epoxy resin. The absorbing and scattering properties of tissue-equivalent phantoms were simulated using microparticles [12–15] of China ink and titanium dioxide, respectively. Mechanical properties of phantoms were simulated by using a two-component silicone gel with different percentages of silicon. Phantoms differed from each other in shape, optical and mechanical properties [9, 12–14]: phantoms with a randomly inhomogeneous structure, phantoms with large inhomogeneity, triple-layer phantoms, phantoms with bifurcations, etc.

Structural OCT images were obtained using an optical fiber interferometer with an electro-optical piezo-fiber depth scanning "OCT 1300-E" (Biomedtech, Nizhny Novgorod, Russia). OCT images of the internal structure of the randomly inhomogeneous blood vessel wall phantom before (a) and after (b) deforming impact are shown in Fig. 1. Dimensions of images are $2,2 \times 1,1$mm., spatial resolution are approximately equal 15 microns.

The key steps of structural OCT images (Fig. 1) processing are shown in Fig. 2 and Fig. 3. The steps of morphological processing of the displacement map and the generation of a convex hull for are shown on the example of displacements of only the light areas (Fig. 2) of the OCT images of the deformed blood vessel wall phantom relative to the OCT image of its initial state.

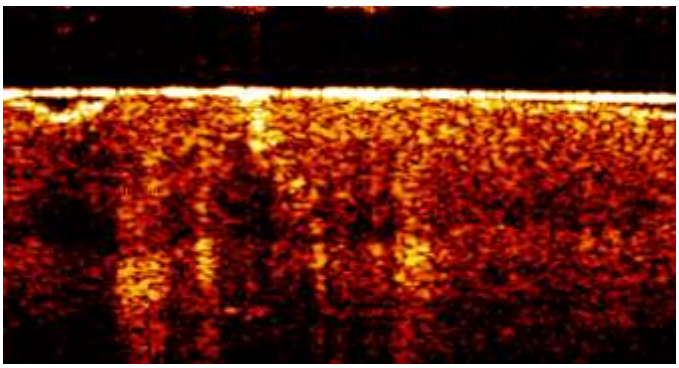

(a)

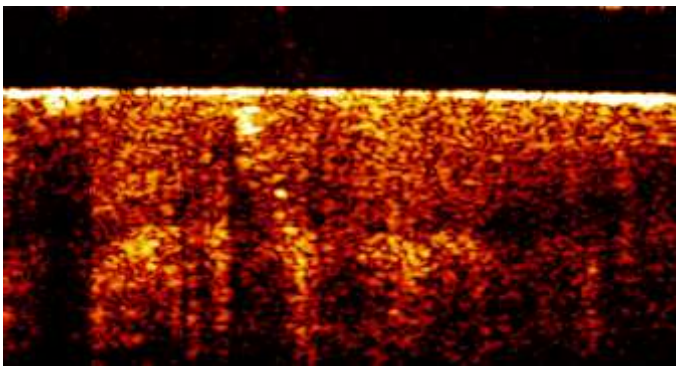

(b)

Fig. 1. Structural OCT images of soft biological tissue phantom before (a) and after (b) the compression

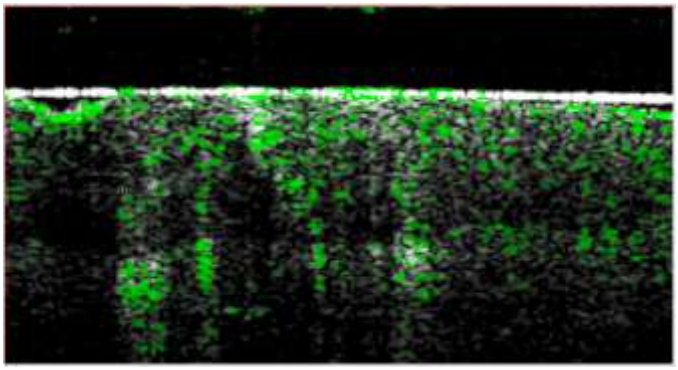

(a)

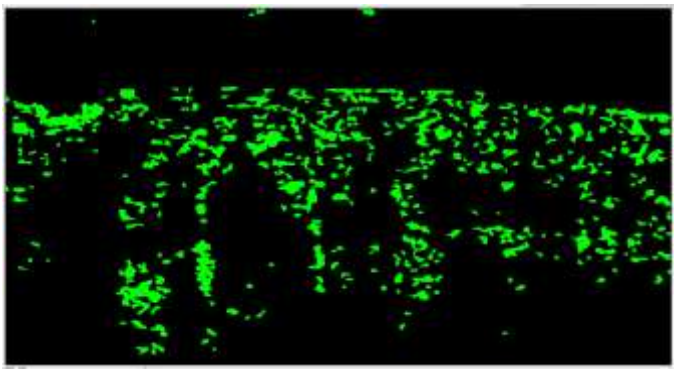

(b)

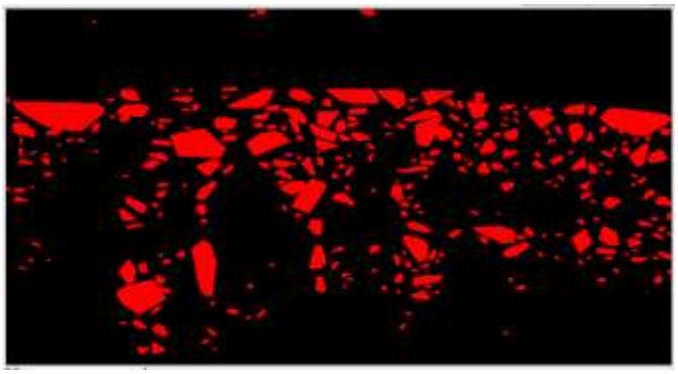

(c)

Fig. 2. Displacements of lighter areas on OCT images of the soft biological tissue phantom (a), the same displacements after the threshold limitation and removal of the border displacements (b), and corresponding convex hulls (c)

The total displacements (Fig. 3a) are the result of the complexation of the displacement cartograms of light (Fig. 2a) and dark areas of OCT images.

The convex hulls of the displacement maps of the light (Fig. 2c) and dark areas are processed using the FAST (Features from Accelerated Segment Test) algorithm. The result of this processing is the test pixels (Fig. 3b), grouping them into pairs using the SURF (Speeded Up Robust Features) algorithm allows to find quantitative values of the displacements in the investigated phantom.

A series of experiments with blood vessel phantoms are showed that the proposed method of Young's modulus and Poisson's ratio estimation using structural OCT images is highly reliable [9]. The average values of Young's modulus and the Poisson's ratio for various blood vessel wall phantoms were found to be: $E_{avr} = 0,992$ MPa and $\mu_{avr} = 0,482$, respectively. Such result corresponds to actual clinical data [16–18]. However, there is a limitation on the usage of the proposed method. The diameter of the investigated vessel should be at least twice the diameter of the forward-side endoscopic probe of the OCT system.

The foregoing means that the proposed method is suitable for diagnosing relatively large blood vessels (diameter more than 4 mm). However, this limitation cannot be called critical [9], so the stress-related properties of the blood vessel should be evaluated in cases of any surgical manipulation, for example, a flow diverter deployment (blood vessels with miliary aneurysm usually unalter).

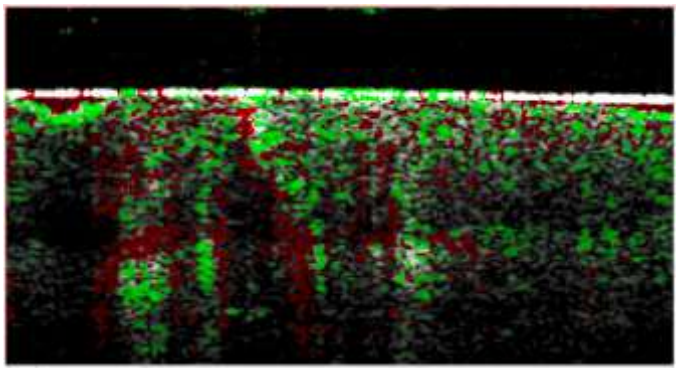

(a)

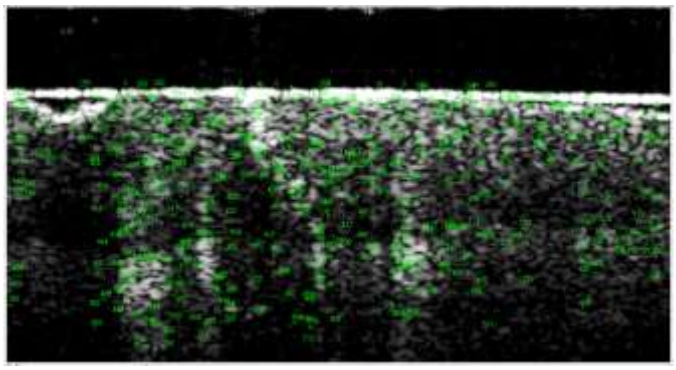

(b)

Fig. 3. Cumulative displacements of light and dark areas on OCT images of the soft biological tissue phantom (a), test points (b) characterizing the cumulative displacements

IV. CONCLUSION

Thus, the original method for increasing the efficiency and reliability of the stress-related properties evaluation for blood vessels using strain elastography based on endoscopic OCT is proposed. Key features of the described method for the Young's modulus and the Poisson's ratio evaluation of a blood vessel wall is application of a pulse wave as a deforming force and analysis of structural OCT images before and after compression using test points for a set of convex hulls. A series of experiments with blood vessel phantoms have demonstrated that values of stress-related properties are in good agreement with the real clinical data [15–18].

REFERENCES

[1] Wang S., Larin K.V. Optical coherence elastography for tissue characterization: a review. *Journal of Biophotonics*, 2015, Vol. 8, Is. 4, pp. 279-302.

[2] Adie S.G., Liang X., Kennedy B.F., John R., Sampson D.D., Boppart S.A. Spectroscopic optical coherence elastography. *Optics Express*, 2010, Vol. 18., Is. 25., pp. 25519-25534.

[3] Gora M.J., Suter M.J., Tearney G.J., Li X. Endoscopic optical coherence tomography: technologies and clinical applications. *Biomedical Optics Express*, 2017, Vol. 8, Is. 5, pp. 2405-2444.

[4] Tsai T.-H., Potsaid B., Tao Y.K., Jayaraman V., Jiang J., Heim P.J.S., Kraus M.F., Zhou C., Hornegger J., Mashimo H., Cable A.E., Fujimoto J.G. Ultrahigh speed endoscopic optical coherence tomography using micromotor imaging catheter and VCSEL technology. *Biomedical Optics Express*, 2013, Vol. 4, Is. 7, pp. 1119-1132.

[5] Li X., Yin J., Hu C., Zhou Q., Shung K.K., Chen Z. High-resolution coregistered intravascular imaging with integrated ultrasound and optical coherence tomography probe. *Applied Physics Letters*, 2010, Vol. 97, Is. 13, No. 133702.

[6] Uribe-Patarroyo N., Bouma B.E. Rotational distortion correction in endoscopic optical coherence tomography based on speckle decorrelation. *Optics Letters*, 2015, Vol. 40, Is. 23, pp. 5518-5521.

[7] Liang S., Saidi A., Jing J., Liu G., Li J., Zhang J., Sun C., Narula J., Chen Z. Intravascular atherosclerotic imaging with combined fluorescence and optical coherence tomography probe based on a double-clad fiber combiner. *Journal of Biomedical Optics*, 2015, Vol. 17, Is. 7., No. 0705011.

[8] Tsai, T.-H., Fujimoto J.G., Mashimo H. Endoscopic optical coherence tomography for clinical gastroenterology. *Diagnostics (Basel)*, 2014, Vol. 4., Is. 2., pp. 57-93.

[9] Frolov S.V., Potlov A.Yu., Sindeev S.V. Selection of flow-diverter stent models using optical coherence tomography and mathematical modeling of hemodynamics. *Biomedical Engineering*, 2018. Vol. 51, Is. 6, pp. 381-384.

[10] Potlov A.Yu., Frolov S.V., Proskurin S.G. An algorithm for improving the quality of structural images of turbid media in endoscopic optical coherence tomography. *Optical Technologies in Biophysics and Medicine XIX - Proceedings of SPIE*, 2018. Vol. 10716, No. 1071609.

[11] Lamouche G., Kennedy B.F., Kennedy K.M., Bisaillon C.E., Curatolo A., Campbell G., Pazos V., Sampson D. Review of tissue simulating phantoms with controllable optical, mechanical and structural properties for use in optical coherence tomography. *Biomedical Optics Express*, 2012, Vol. 3., Is. 6., pp. 1381-1398.

[12] Pogue B.W., Patterson M.S. Review of tissue simulating phantoms for optical spectroscopy, imaging and dosimetry. *Journal of Biomedical Optics*, 2006, Vol. 11, Is. 4, No. 041102.

[13] Bashkatov A.N., Genina E.A., Tuchin V.V. Optical properties of skin, subcutaneous, and muscle tissues. *Journal of Innovative Optical Health Sciences*, 2011, Vol. 4., pp. 9-38.

[14] Frolov S.V., Potlov A.Yu., Petrov D.A., Proskurin S.G. Modelling of a structural image of a biological object obtained by means of optical coherent tomography using the Monte Carlo method based on the voxel geometry of a medium. *Quantum Electronics*, 2017, Vol. 47, Is. 4, pp. 347-354.

[15] Khalil A.S., Chan R.C., Chau A.H., Bouma B.E., Mofrad M.R.K. Tissue elasticity estimation with optical coherence elastography: toward mechanical characterization of *in vivo* soft tissue. *Annals of Biomedical Engineering*, 2005, Vol. 33, pp. 1631-1639.

[16] Chan R.C., Chau A.H., Karl W.C., Nadkarni S., Khalil A.S., Iftimia N., Shishkov M., Tearney G.J., Kaazempur-Mofrad M.R., Bouma B.E. OCT-based arterial elastography: robust estimation exploiting tissue biomechanics. *Optics Express*, 2004, Vol. 12, pp. 4558-4572.

[17] Rogowska J., Patel N.A., Fujimoto J.G., Brezinski M.E. Optical coherence tomographic elastography technique for measuring deformation and strain of atherosclerotic tissues. *Heart*, 2004, Vol. 90, Is. 5, pp. 556-562.

[18] Lasheras J.C. The biomechanics of arterial aneurysms. *Annual Review of Fluid Mechanics*, 2007, Vol. 39, pp. 293-319.